Journal of Applied Polymer Science

# Melt Rheological Properties of PBT/SEBS and Reactively Compatibilized PBT/SEBS/SEBS-*g*-MA Polymer Blends

**Rajul Sharma, Saurindra Nath Maiti**
Centre for Polymer Science and Engineering, Indian Institute of Technology, New Delhi, India
Correspondence to: S. N. Maiti (E-mail: sharma_rajul@rediffmail.com or maitisn49@yahoo.co.in)

**ABSTRACT:** Melt rheological properties of PBT/SEBS and PBT/SEBS/SEBS-*g*-MA blends at SEBS volume fraction ($\Phi_d$) = 0.00–0.38 were studied at 240°C, 250°C and 260°C using a capillary rheometer. The compatibilizer SEBS-*g*-MA addition resulted in significant reduction in the dynamic interfacial tension which in turn led to increased phase adhesion. The power law exponent n decreased with increasing $\Phi_d$ and increasing temperature for both the compatiblized and uncompatiblized blends. The consistency index of PBT/SEBS increased with increasing $\Phi_d$ but were smaller than those of PBT/SEBS/SEBS-*g*-MA blends. Melt elasticity such as die swell and first normal stress difference increased with $\Phi_d$. Variations of first normal stress coefficient function ($\psi_1$), recoverable shear strain ($\gamma_R$), relaxation time ($\lambda$), and shear compliance ($J_c$) values versus shear rate were analyzed. © 2014 Wiley Periodicals, Inc. J. Appl. Polym. Sci. **2015**, *132*, 41402.

**KEYWORDS:** blends; compatibilization; rheology; viscosity; viscoelasticity

Received 8 July 2013; accepted 14 August 2014
**DOI: 10.1002/app.41402**

## INTRODUCTION

One of the most important procedures to modify and improve the properties of a polymer is its blending with one or several other polymers. Most commercial multicomponent polymer systems are two phase blends that provide advantages over the single phase systems.[1,2] The toughening of a brittle plastic via blending with an elastomer constitutes a convincing example.[3] The concentration, particle size, and properties of the elastomer as well as the interaction between phases determine the mechanical and rheological properties of the toughened plastics.[4–6]

Poly(butylene terephthalate), PBT, is an aromatic polyester with a rapid crystallization rate that finds uses as an engineering material due to its attractive mechanical properties, good moldability, excellent electrical insulation, and dimensional stability.[7,8] However, due to the polymer's low notched impact strength it is often blended with several types of elastomers and related polymers. On the basis of its structure PBT is capable of chemical reactions and of specific polar interactions like H-bonding with polar polymers.

PBT and styrene-ethylene-butylene-styrene (SEBS) polymer are incompatible and their blends show, in general, poor properties. Compatibilization is then a necessary step to obtain blends with good balance of tensile modulus and strength vis-a-vis notched izod impact properties. Generally, compatibilizers consist of graft or block copolymers with different segments possessing affinity for one or the other of the blend components. It has been established that graft or block copolymers can effectively decrease the interfacial tension between the components, improve phase dispersion and result in fine and stable morphology.[9] The compatibilized blends show a dramatic change of the morphology, an enhancement of the viscosity and a significant improvement of the mechanical properties with respect to the uncompatibilized binary blend.

Styrene-ethylene-butylene-styrene (SEBS) triblock copolymer was shown to enhance impact properties of PBT.[10] Crystallinity decreased along with tensile modulus and strength, however, elongation at break enhanced significantly. In this blend the maleic anhydride grafted SEBS (SEBS-*g*-MA) functions as a compatibilizer giving rise to fine and stable phase morphology. The hydrocarbon blocks are miscible with PBT while the MA-containing moieties may interact with PBT. Grafting with MA increases the polarity of the ethylene/butylenes (E/B) blocks thus effecting the interaction with PBT. The above block copolymers are thermoplastic elastomers that can flow at high temperature and behave as a crosslinked rubber at low temperature. Their use as impact modifier in a number of polymer blends was examined by Lu et al.[11,12]

Rheology is one of the most frequently used methods for characterizing the interfacial properties of polymers and the rheological properties of immiscible polymer blends have been studied extensively. Rheological properties offer a deep insight

into the flow dynamics of the elastomer dispersed systems under the processing conditions and open up a technologically feasible processing window suitable for processing the materials to attain the desired morphology to acquire fine tailorable end-properties. Also, reactive compatibilization of polymer blends exhibits significant impact on rheological properties.[13,14] Rheological properties PBT/ASA/Epoxy,[15] PBT/ABS/ASMA,[16] and PBT/thermoplastic elastomer[17] blends have been reported.

The use of SEBS as the blending phase in PBT may enhance the oxidation stability of the blends since SEBS has no residual unsaturation. Also, there is no literature report on the rheological properties of these blends. The aim of the work is thus to evaluate the rheological behavior of the blends which help in setting up processing parameters.

In this article, melt rheological properties of PBT/SEBS blends were studied at the blending polymer volume fraction ($\Phi_d$) 0 to 0.38 at three temperatures viz., 240°C, 250°C and 260°C. The rheological parameters e.g., shear stress-shear rate variation, apparent melt viscosity, power law index, flow consistency coefficient as well as melt elasticity parameters were evaluated and analyzed. A piston-type capillary rheometer was used to generate the rheological parameters. The effects of using a phase compatibilizer, SEBS-*g*-MA copolymer, on the above parameters have also been examined.

## EXPERIMENTAL

### Materials

PBT (Crastin® 6129NC010, density 1.31 g/mL) was procured from the DuPont Engineering Polymer. SEBS (Kraton G1651, density 0.91 g/mL, 67 wt (%) of ethylene–butylene block and 33 wt (%) of styrene block) from Shell chemical Company, was used as the minor component. SEBS-*g*-MA (Kraton FG 1901X) containing maleic anhydride content 1.7 to 2.0 wt % was used as compatibilizer. The compatibilizer content was 5 wt % of the SEBS.

### Compounding

Granules of PBT, SEBS, and SEBS-*g*-MA copolymers were vacuum dried at 110°C for 4 h. The components were first tumble mixed and then melt compounded on a co-rotating twin screw extruder, Model JSW J75EIV-P ($L/D = 36$, diameter = 30 mm) at 250 rpm. From the feed zone to the die zone the temperature varied from 195°C to 250°C. The extruded strands were chilled in cold water, pelletized and vacuum dried at 110°C for 4 h. These pellets were fed to the rheometer to generate the melt flow parameters. Individual polymers were also extruded under identical conditions to ensure the same thermal and shear history as that of the blend compositions. The blend compositions were expressed as volume fractions of the dispersed phase, $\Phi_d$, calculated from the mass and density values of the components in the blend.[10]

### Compression Molding

Compression molding was done to make circular disc for parallel plate rheology test using Carver Inc, auto series compression moulding machine. The molding conditions were temperature: 250°C, pressure: 13,000 lb, heating time: 2-min heating under pressure, followed by 2 min breathing and finally 5 min heating and followed by cooling under pressure at a rate of 13.5°C/min up to 120°C.

### Dynamic Oscillatory Rheology

Parallel plate rheological tests were performed using Bohlin C-VOR instrument. Dynamic frequency time sweep tests were employed to look for any changes with time in their complex viscosity over time at a constant frequency (1 rad/s) and at 250°C temperature.

### Measurements

A piston-type capillary rheometer was used to generate the rheological parameters such as shear stress, shear rate, apparent melt viscosity, and the melt elasticity at SEBS concentrations from 0 to 0.38 volume fractions. The samples were dried at 100°C for 4 h under vacuum prior to measurements. The rheological properties were measured at three temperatures, 240°C, 250°C, and 260°C, in the shear rate range 100 $s^{-1}$ to 5000 $s^{-1}$ on a Rosand Advanced Rheometer system dual bore capillary rheometer. The capillary rheometers suggest the flow behavior in the common important polymer processing, e.g., extrusion and injection molding. The $L/D$ ratio of the capillary in one bore was 16/1 whereas the orifice die in another bore was a zero length capillary. The application of two capillary system permits standard Bagley and Rabinowitsch corrections automatically during the measurements.[18,19]

The results were processed by the software provided by the Malvern Instrument Ltd.[18] The apparent shear rate, $\dot{\gamma}_a$, was calculated following eq. (1):[20–23]

$$\dot{\gamma}_a = \left(\frac{4Q}{\Pi R^3}\right) \ (s^{-1}) \tag{1}$$

where $R$ is the capillary die radius (cm) and $Q$ is the volumetric flow rate ($cm^3\ s^{-1}$) given by:

$$Q = AS/t = Av \ (cm^3 s^{-1}) \tag{2}$$

where $v$ is the piston speed ($cms^{-1}$), $A$ the area ($cm^2$), $S$ the piston path (cm) and $t$ the time (s).

The true shear rate at the wall of the capillary, $\dot{\gamma}_W$, was calculated using the $\dot{\gamma}_a$ values by applying the Rabinowitsch- Weissenberg correction:[22,24,25]

$$\dot{\gamma}_w = \left(\frac{3n+1}{4n}\right)\dot{\gamma}_a (s^{-1}) \tag{3}$$

where $n$ is the flow behavior index (also known as the power law exponent) obtained from the slope of the logarithmic plots of the shear viscosity ($\eta_a$) versus shear rate $\dot{\gamma}_W$. For Newtonian behavior, $n = 0$, and values of $n<1$ denote pseudoplastic (thermoplastics) shear thinning behavior, while values $n>1$ imply shear- thickening characteristics. Generally for polymers the values of $n$ are from 0.8 to 0.2. The apparent melt shear viscosity, $\eta_a$, is calculated by the rheometer instrument software, Flow Master Analysis, using the relation in eq. (4):[24,25]

$$\eta_a = K\dot{\gamma}_w^{(n-1)} \tag{4}$$

The relation between $\zeta_w$ and $\dot{\gamma}_W$ is given by the "Power law (Ostwald-de waele)"where $K$ is the consistency index, eq. (5):

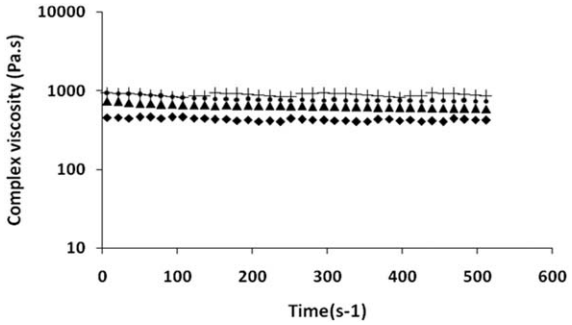


**Figure 1.** Variation of complex viscosity of neat PBT (◆), extruded PBT (▲), un-compatibilized, (•) and compatibilized (+) blends at $\Phi_d = 0.26$, versus time.

$$\tau_w = K\dot{\gamma}_w^{(n)} \quad (5)$$

Extrudate swell ratio was evaluated following eq. (6):

$$\text{Extrudate swell ratio} = [D_i/D] \quad (6)$$

where $D_i$ is the diameter of the extrudate and $D$ the diameter of the capillary die. The extrudates were snapped after exit from the die as 5 cm long strands. The diameters were measured at several places by using a micrometer after standing the strands for 24 h.

### Influence of Temperature on Melt Viscosity

An exponential dependence of viscosity on temperature can be expressed by the semilogarithmic Arrhenius equation:[23,26]

$$\eta_a = Ae^{(\Delta E/RT)} \quad (7)$$

where $A$ is a constant characteristic of the polymer, $T$ the absolute temperature, $\Delta E$ the activation energy for viscous flow, and $R$ the universal gas constant (8.314 KJ/mol).[24] The activation energy of the viscous flow was calculated from the slope of the log $\eta_a$ versus $1/T$ plots.

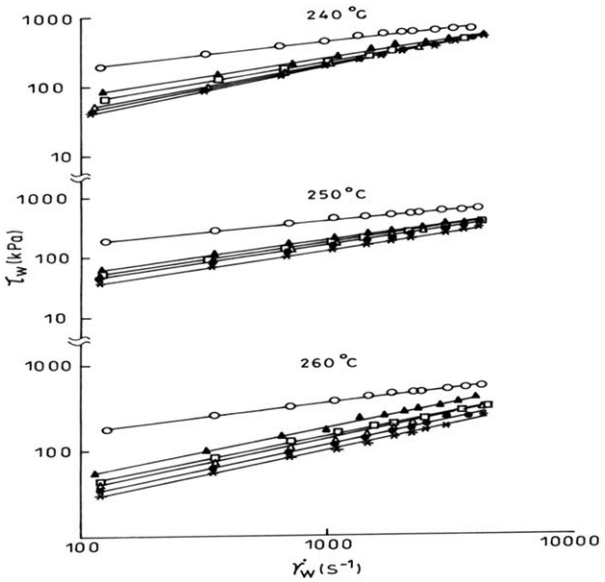


**Figure 2.** Variations of $\tau_w$ against $\dot{\gamma}_w$ at 240°C, 250°C, and 260°C in PBT/SEBS blends at varying $\Phi_d$ values: (×) 0, (•) 0.07, (Δ) 0.14, (□) 0.26, (▲) 0.38, and (○) 1.

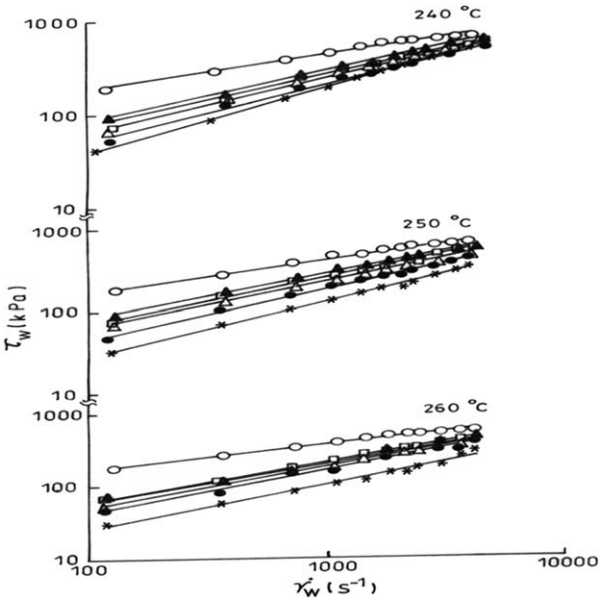


**Figure 3.** Variations of $\zeta_w$ against $\dot{\gamma}_w$ at 240°C, 250°C, and 260°C in PBT/SEBS blends at varying $\Phi_d$ values: (×) 0, (•) 0.07, (Δ) 0.14, (□) 0.26, (▲) 0.38, and (○) 1.

## RESULTS AND DISCUSSION

### Dynamic Oscillatory Rheology

Dynamic frequency time sweep tests were employed to look for any changes with time in their complex viscosity over time at a constant frequency (1 rad/s) and at 250°C temperature. The blending time was ~100 s. As it can be seen in Figure 1, all melt samples had nearly constant complex viscosity up to 300 s showing thermal stability up to that time. This implies that neither PBT nor the blends degrade during the extrusion blending of the samples.

### Shear Stress ($\tau_w$)–Shear Rate ($\dot{\gamma}_W$) Variations

Figure 2 shows the logarithmic plots of the shear stress ($\tau_w$) versus shear rate ($\dot{\gamma}_W$) at temperatures, 240°C, 250°C, and 260°C for the PBT/SEBS blends. The variations were linear in the shear rate range studied (100–5000 $s^{-1}$). The shear stress increases with $\Phi_d$ and also with shear rate which indicates that the blends followed power law behavior similar to other filled polymer and blend systems.[27] As SEBS concentration increased, the flow curves moved upward. This means that at a constant shear rate a system with high SEBS concentration shows higher shear stress than a blend with low SEBS content.

For the PBT/SEBS/SEBS-*g*-MA blends, the logarithmic plots of $\tau_w$ versus $\dot{\gamma}_W$ at 240°C, 250°C, and 260°C are shown in Figure 3. The flow curves are similar to those of the PBT/SEBS blends, however, the values of the shear stress are to an extent higher at corresponding temperatures. The SEBS-*g*-MA is of low molecular weight than the SEBS polymer but in all the compositions SEBS content is much higher than SEBS-*g*-MA copolymer content. The enhanced phase adhesion effect resulting in higher shear stress includes the contributions of both the stronger

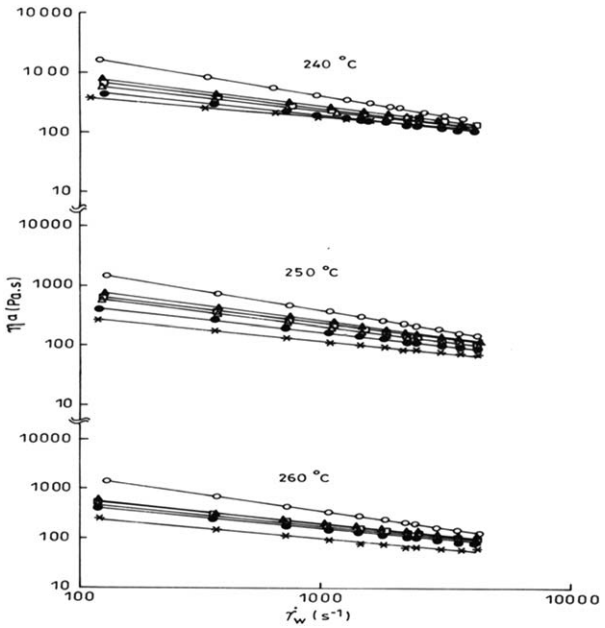


**Figure 4.** Plots of melt viscosity ($\eta_a$) versus shear rate $\dot{\gamma}_w$ at 240°C, 250°C and 260°C in PBT/SEBS blends at varying $\Phi_d$ values: (×) 0, (•) 0.07, (Δ) 0.14, (□) 0.26, (▲) 0.38, and (○) 1.

interfacial adhesion and the finer phase morphology of the blends.

### Melt Viscosity

**PBT/SEBS Blends.** Melt shear viscosity results of PBT/SEBS blends at varying volume fraction of the blending polymer in the shear rate range 100 $s^{-1}$ to 5000 $s^{-1}$ and at 240°C, 250°C, and 260°C, are presented in Figure 4. At all temperatures the SEBS copolymer possesses higher shear viscosity than PBT in the shear rate range studied and the $\eta_a$ values of the blends lie in between those of PBT and SEBS.

The $\eta_a$ data increase with SEBS content compared to that of PBT. The increase in viscosity of the blends may be due to enhanced entanglement caused by the interdiffusion of the butylenes sequences of PBT and ethylene-butylene component of SEBS copolymer as was reported in the static mechanical property of the blends.[10] At low shear rate regions (200 $s^{-1}$ to 1000 $s^{-1}$), this chain entanglement restricted the flow causing increased melt viscosity while at higher shear rates the molecules tend to disentangle easily under the action of enhanced viscous forces. Also in this low shear rate range, the separation of the curves was more prominent, which may be attributed to the relative predominance of extensional flow over shear flow of PBT in presence of SEBS particles. Extensional flow is significant at low $\dot{\gamma}_W$ values up to 1000 $s^{-1}$ whereas at higher $\dot{\gamma}_W$ values shear flow takes prominence.[28,29] Since the phases are entangled the blends do not exhibit interfacial slip in the shear flow.

At ~3000 $s^{-1}$ shear rate of injection molding of the blends the viscosity ratio ($\eta_r$) of the discrete phase to that of the matrix ($\eta_{SEBS}/\eta_{PBT}$) is 1.4, 2.3, and 2.51, at 240°C, 250°C, and 260°C, respectively. The values of $\eta_r$ are ≤2.5 suggesting that the elastomer phase dispersion could be stable in the matrix phase as proposed by Taylor and other researchers.[30,31] This was indeed observed in the morphology of the PBT/SEBS blends processed at 250°C.[10] Similar kind of spherical domains of the minor phase dispersed in the matrix was observed in PS/PPO, PE/PA6, and other systems also where the viscosity of the minor phase is less than that of the continuous phase.[32,33]

**Table I.** Viscosity Functions of the Uncompatibilized PBT/SEBS Blends

| Volume fraction ($\Phi_d$) | Temp (°C) | Viscosity function, $\eta = K\,\dot{\gamma}^{(n-1)}$ | $R^2$ | Power law index ($n$) | Flow consistency index ($K$) |
|---|---|---|---|---|---|
| 0 | 240 | $\eta = 1{,}615\,\dot{\gamma}^{0.69-1}$ | 0.995 | 0.69 | 1,615 |
| 0.07 | 240 | $\eta = 2{,}149\,\dot{\gamma}^{0.65-1}$ | 0.988 | 0.65 | 2,149 |
| 0.14 | 240 | $\eta = 2{,}911\,\dot{\gamma}^{0.6-1}$ | 0.999 | 0.6 | 2,911 |
| 0.26 | 240 | $\eta = 4{,}742\,\dot{\gamma}^{0.55-1}$ | 0.989 | 0.55 | 4,742 |
| 0.38 | 240 | $\eta = 7{,}286\,\dot{\gamma}^{0.51-1}$ | 0.993 | 0.51 | 7,286 |
| 1 | 240 | $\eta = 36{,}030\,\dot{\gamma}^{0.36-1}$ | 0.993 | 0.36 | 36,030 |
| 0 | 250 | $\eta = 1{,}720\,\dot{\gamma}^{0.62-1}$ | 0.991 | 0.62 | 1,720 |
| 0.07 | 250 | $\eta = 3{,}030\,\dot{\gamma}^{0.57-1}$ | 0.99 | 0.57 | 3,030 |
| 0.14 | 250 | $\eta = 3{,}294\,\dot{\gamma}^{0.57-1}$ | 0.999 | 0.57 | 3,294 |
| 0.26 | 250 | $\eta = 3{,}563\,\dot{\gamma}^{0.56-1}$ | 0.977 | 0.56 | 3,563 |
| 0.38 | 250 | $\eta = 4{,}866\,\dot{\gamma}^{0.53-1}$ | 0.995 | 0.53 | 4,866 |
| 1 | 250 | $\eta = 34{,}235\,\dot{\gamma}^{0.35-1}$ | 0.993 | 0.35 | 34,235 |
| 0 | 260 | $\eta = 1{,}852\,\dot{\gamma}^{0.58-1}$ | 0.982 | 0.58 | 1,852 |
| 0.07 | 260 | $\eta = 2{,}150\,\dot{\gamma}^{0.58-1}$ | 0.985 | 0.58 | 2,150 |
| 0.14 | 260 | $\eta = 2{,}713\,\dot{\gamma}^{0.57-1}$ | 0.988 | 0.57 | 2,713 |
| 0.26 | 260 | $\eta = 3{,}436\,\dot{\gamma}^{0.54-1}$ | 0.982 | 0.54 | 3,436 |
| 0.38 | 260 | $\eta = 3974\,\dot{\gamma}^{0.56-1}$ | 0.995 | 0.56 | 3,974 |
| 1 | 260 | $\eta = 34212\,\dot{\gamma}^{0.33-1}$ | 0.995 | 0.33 | 34,212 |

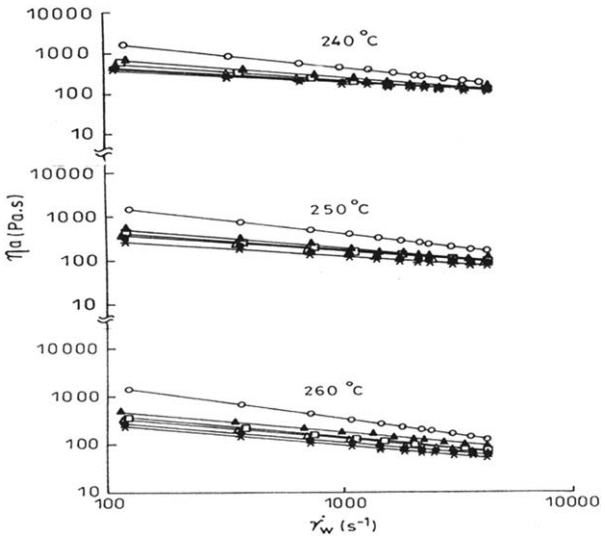


**Figure 5.** Plots of melt viscosity ($\eta_a$) versus shear rate $\dot{\gamma}_w$ at 240°C, 250°C, and 260°C in PBT/SEBS/SEBS-*g*-MA blends at varying $\Phi_d$ values: (×) 0, (•) 0.07, (Δ) 0.14, (□) 0.26, (▲) 0.38 and (○) 1.

The melt viscosities of the blends were higher than that of PBT, the value increased with increasing $\Phi_d$, the parameter decreased to an extent with increasing temperature for PBT/SEBS blends.

The melt viscosities of the blends were higher than that of PBT, the value increases with $\Phi_d$ which may be due to enhanced entanglement of PBT with SEBS chains. The melt viscosities decrease with increase in temperature which is ascribed to lesser resistance to flow at higher temperature since intermolecular attraction forces are overcome.

At all temperatures and higher shear rate the $\eta_a - \dot{\gamma}_W$ curves tend to converge which indicates that the variation of SEBS content and its resultant entanglement with PBT is overcome at very high shear rates, the entanglement effect is reduced as in all the thermoplastics.

Power law model, eq. (4), was used to evaluate the viscosity function $\eta_a$, power law index $n$, and flow consistency parameter $K$ in the PBT/SEBS blends, Table I. The parameter $n$ describes the extent of non-newtonian behavior, the lesser the value from

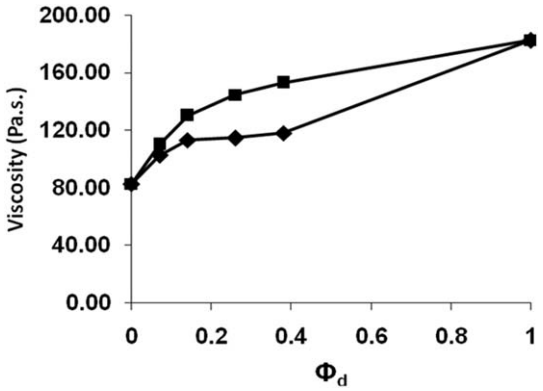


**Figure 6.** Variation of melt viscosity versus $\Phi_d$ in the PBT/SEBS blends (◆) and PBT/SEBS/SEBS-*g*-MA blends (■) at 250°C.

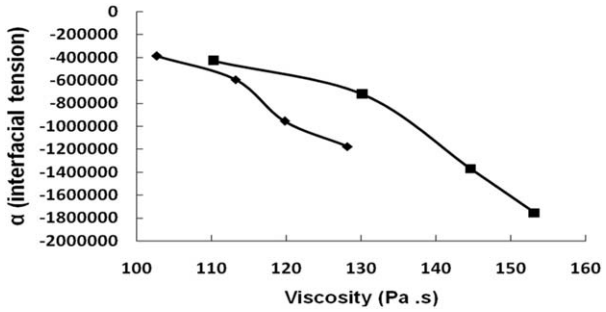


**Figure 7.** Variation of interfacial tension (α) versus viscosity in the PBT/SEBS (◆) and PBT/SEBS/SEBS-*g*-MA blends (■) at 250°C.

unity the higher the non-Newtonian property of the molten polymer. For a shear thinning fluid $n < 1$, a decrease in $n$ gives rise to an exponential increase in flow. At all the temperatures the binary blends exhibit decrease in the $n$ values with increase in $\Phi_d$, implying an enhancement or ease of flow of PBT on addition of SEBS copolymer. At any $\Phi_d$, the $n$ value decreases with increase in temperature which is due to enhanced flow at higher temperatures.

The variable $K$ denotes flow consistency index which describes increase in resistance to flow of the fluid. At all the temperatures, the value of $K$ increases with $\Phi_d$ which indicates that the elastic recovery of the melt may enhance at higher $\Phi_d$ values which in turn increases the resistance to flow.[31] The $K$ values enhance up to 250°C showing a maximum and then decrease at 260°C. At 260°C, the values are even lower than those at 240°C. It implies that elastic recovery increases due to enhanced phase interaction reaching a maximum value at 250°C. The parameter decreases upon further increase in temperature due probably to decrease in phase adhesion.

### Compatibilized PBT/SEBS Blends with SEBS-*g*-MA Copolymers

The shear viscosity-shear strain plots of reactively compatibilized PBT/SEBS blends at varying contents of SEBS (SEBS-*g*-MA at 5% of SEBS) are shown in Figure 5. Here also, the $\eta_a$ data for the blends were higher than that of PBT and lower than that of SEBS, the data were marginally higher than those of PBT/SEBS blends, however. This may be to phase interaction between PBT and SEBS-*g*-MA through chemical/physical bonding arising out of carboxylic acid groups of MA and —OH end groups of PBT[10] which increases the viscosity of the system. A network type of structure can form which enhances the friction for the polymer melt flow. In other systems also, phase interaction was observed to enhance the melt viscosity.[27,29]

With increase in shear rate the compatibilized blends also exhibited decrease in $\eta_a$ and beyond 3500 $s^{-1}$ the curves tend to converge implying marginal effect of phase interaction at high viscous forces, Figure 5. It implies that reactive compatibilization decreases interfacial slip in PBT/SEBS/SEBS-*g*-MA blend systems.

The melt viscosity is plotted versus $\Phi_d$ at 250°C and a fixed shear rate 3000 $s^{-1}$, Figure 6, which shows that the viscosity enhanced to an extent in the uncompatibilized blend which

**Table II.** Viscosity Functions of the Compatibilized PBT/SEBS/SEBS-*g*-MA Blends

| Volume fraction ($\varphi_d$) | Temp (°C) | Viscosity function $\eta = K\,\dot{\gamma}^{(n-1)}$ | $R^2$ | Power law index ($n$) | Flow consistency index ($K$) |
|---|---|---|---|---|---|
| 0 | 240 | $\eta = 1{,}615\,\dot{\gamma}^{0.69-1}$ | 0.995 | 0.69 | 1,615 |
| 0.07 | 240 | $\eta = 3{,}312\,\dot{\gamma}^{0.6-1}$ | 0.977 | 0.6 | 3,312 |
| 0.14 | 240 | $\eta = 4{,}819\,\dot{\gamma}^{0.56-1}$ | 0.992 | 0.56 | 4,819 |
| 0.26 | 240 | $\eta = 6{,}554\,\dot{\gamma}^{0.7-1}$ | 0.981 | 0.53 | 6,554 |
| 0.38 | 240 | $\eta = 7{,}600\,\dot{\gamma}^{0.7-1}$ | 0.998 | 0.53 | 7,600 |
| 1 | 240 | $\eta = 36{,}030\,\dot{\gamma}^{0.36-1}$ | 0.993 | 0.36 | 36,030 |
| 0 | 250 | $\eta = 1{,}720\,\dot{\gamma}^{0.62-1}$ | 0.991 | 0.62 | 1,720 |
| 0.07 | 250 | $\eta = 3{,}380\,\dot{\gamma}^{0.57-1}$ | 0.992 | 0.57 | 3,380 |
| 0.14 | 250 | $\eta = 6{,}225\,\dot{\gamma}^{0.50-1}$ | 0.995 | 0.5 | 6,225 |
| 0.26 | 250 | $\eta = 6{,}338\,\dot{\gamma}^{0.53-1}$ | 0.988 | 0.53 | 6,338 |
| 0.38 | 250 | $\eta = 8{,}933\,\dot{\gamma}^{0.49-1}$ | 0.995 | 0.49 | 8,933 |
| 1 | 250 | $\eta = 34{,}235\,\dot{\gamma}^{0.35-1}$ | 0.993 | 0.35 | 34,235 |
| 0 | 260 | $\eta = 1{,}701\,\dot{\gamma}^{0.59-1}$ | 0.965 | 0.59 | 1,701 |
| 0.07 | 260 | $\eta = 3{,}110\,\dot{\gamma}^{0.57-1}$ | 0.966 | 0.57 | 3,110 |
| 0.14 | 260 | $\eta = 4{,}181\,\dot{\gamma}^{0.55-1}$ | 0.988 | 0.55 | 4,181 |
| 0.26 | 260 | $\eta = 5{,}357\,\dot{\gamma}^{0.53-1}$ | 0.995 | 0.53 | 5,357 |
| 0.38 | 260 | $\eta = 5{,}552\,\dot{\gamma}^{0.52-1}$ | 0.958 | 0.52 | 5,552 |
| 1 | 260 | $\eta = 37{,}212\,\dot{\gamma}^{0.33-1}$ | 0.995 | 0.33 | 34,212 |

may be due to interdiffusion of the phases leading to phase adhesion. This indicates that interfacial stick phenomenon is operative in the blends. In the compatibilized blends the $\eta_a$ values are an extent higher implying increased extent of interfacial stick mechanism. The enhancement of melt viscosity of the compatibilized blend indicates that the phase interaction is effective even at a higher temperature 250°C which are higher than the crystalline melting temperature of the crystallizable matrix PBT.

Interfacial tension ($\alpha$), Eq. (8), has been calculated at 250°C from Figure 6 and plotted against viscosity in Figure 7. It can be observed that as the interfacial tension decreases in PBT/SEBS blends the $\eta_a$ increases. This may be due to interdiffusion of butylenes sequences of PBT and ethylene-butylene components of SEBS copolymer as was reported in the solid state mechanical property of the blends.[10]

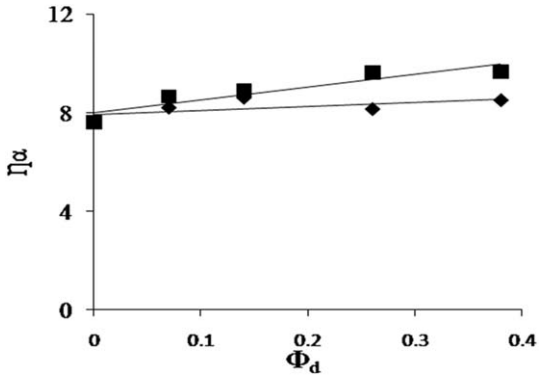


**Figure 8.** Variation of $\eta_\infty$ data versus $\Phi_d$ in the PBT/SEBS (◆) and PBT/SEBS/SEBS-*g*-MA (■) blends.

In the compatibilized blends also as $\alpha$ decreases the viscosity increases and the decrease in $\alpha$ is to an extent higher. This gives an indication of enhanced phase adhesion, i.e. formation of a stronger interphase in presence of the comptibilizer. Thus the viscosity increase with blend composition may be attributed to the increase in phase adhesion. In the morphological studies it was observed that in PBT/SEBS blends the $d_w$ of the dispersed phase varied from 0.69 $\mu$m to 1.04 $\mu$m as $\Phi_d$ varied from 0.07 to 0.38 while for PBT/SEBS/SEBS-*g*-MA blends the elastomer particle size varied from 0.65 $\mu$m to 0.98 $\mu$m. In the compatibilized blend individual particle sizes are to a degree smaller than in the uncompatibilized system. Thus the morphology studies also provide a supportive evidence for phase adhesion in PBT/SEBS and PBT/SEBS/SEBS-*g*-MAblends. Table II shows the viscosity functions of PBT/SEBS/SEBS-*g*-MA blends. The power law indices are marginally lower than the PBT/SEBS blends at corresponding $\Phi_d$ and temperature values which may be due to a partial plasticizing function by the low molecular weight SEBS-*g*-MA fraction produced during MA grafting or degradation of the later during processing. The $K$ values are significantly higher than those in the uncompatibilized blends which may be due to enhanced phase adhesion[10] as was also observed in other works.[27,34]

### Dynamic Interfacial Effects

The discrete phase is a non-Newtonian particle dispersed in the major phase. In such a system particle break up is governed by interfacial effects which in turn are generated by dynamic interfacial viscosities, interfacial elasticities and interfacial tension

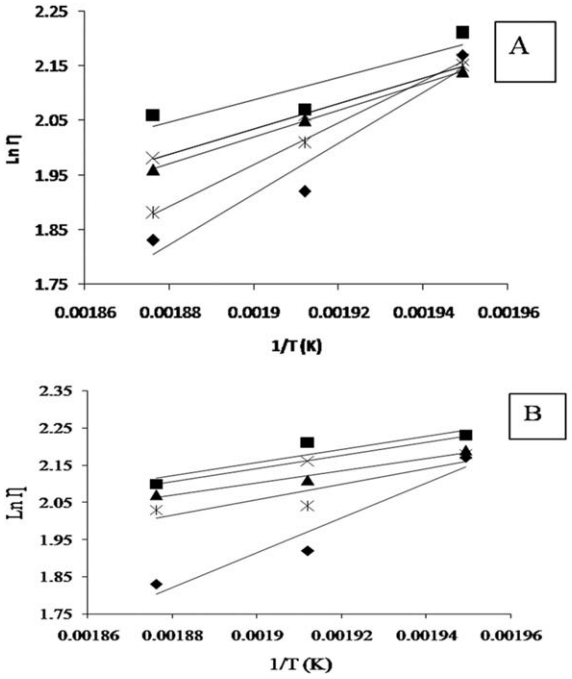


**Figure 9.** Variation of log $\eta$ versus $1/T$ for the (A) PBT/SEBS and (B) PBT/SEBS/SEBS-*g*-MA blends at varying $\Phi_d$ : 0 (◆), 0.07 (∗), 0.14 (▲), 0.26 (×), and 0.38 (■).

gradients. However, these interfacial tension forces are balanced by the normal forces of the matrix. In these calculations assuming the droplets as Newtonian may not represent actual situation. Along with the viscosity ratio and interfacial tension the melt elasticity (normal stresses) of the polymers also controls the particle break up.[31,35] The interfacial tension is in effect dynamic and can be evaluated by balancing the shear forces, continuous phase elasticity, interfacial tension gradient and dispersed phase elasticity. The interfacial tension $\alpha$ can be estimated from eq. (8):

$$\alpha = D(\tau_W - N_1)/2 \tag{8}$$

where $D$ is the minimum volumetric particle size ($\mu_m$), $\tau_w$ the wall shear stress (Pa), and $N_1$ the first normal stress difference (elasticity) (Pa). At injection molding condition i.e. at a fixed shear rate of 3000 $s^{-1}$ the $\alpha$ values calculated for PBT/SEBS blend ($D_v = 0.79$ $\mu$m),[10] $\tau_w = 340{,}390$ Pa, $N_1 = 1{,}773{,}950$ Pa) and for PBT/SEBS/SEBS-*g*-MA blends ($D_v = 0.76$ $\mu$m),[10] $\tau_w = 357{,}900$ Pa, $N_1 = 2{,}224{,}290$ Pa) were −566,250 N/m and −696,800 N/m, respectively. The decrease in the interfacial tension was by ∼23%. This decrease in $\alpha$ value upon addition of the compatibilizer accounts for reduction of dispersed phase diameter in the blends.[10]

**Table III.** Values of the Activation Energy for Viscous Flow ($\Delta E$) for the PBT/SEBS and PBT/SEBS/SEBS-*g*-MA Blends at Shear Rate 2000 $s^{-1}$.

| $\Phi_d$ | PBT/SEBS blends, $\Delta E$ (kJ $mol^{-1}$ $K^{-1}$) | PBT/SEBS/SEBS-*g*-MA blends, $\Delta E$ (kJ $mol^{-1}$ $K^{-1}$) |
|---|---|---|
| 0 | 38.75 | 38.75 |
| 0.07 | 31.83 | 17.13 |
| 0.14 | 20.45 | 13.65 |
| 0.26 | 19.32 | 12.52 |
| 0.38 | 17.13 | 14.70 |

### Viscosity Function Evaluation in the High Shear Range

The viscosity data at high shear range were compared with Casson eq. (9) in order to evaluate material behaviors other than those obtained using power law model:

$$\eta^{1/2} = \eta_\infty{}^{1/2} + \tau_0{}^{1/2}\gamma^{-1/2} \tag{9}$$

where the parameter $\eta_\infty$ describes infinite viscosity where all the rheological structures break down.[36] From the plot of variation of $\eta^{1/2}$ versus $1/\gamma^{1/2}$ the value of $\eta^{1/2}{}_\infty$ is obtained the square of which gives $\eta_\infty$ at infinite shear rate. The square of the slope of the Casson plot, eq. (9), gives Casson yield stress $\tau_0$ which is a measure of shear thinning of the melt. The significance of $\tau_0$ is thus quite similar to the reciprocal of n in the power law model. Beyond $\eta_\infty$ the apparent shear viscosity of a polymer remains unaltered. Figure 8 shows variation of $\eta_\infty$ data versus $\Phi_d$ in the PBT/SEBS and PBT/SEBS/SEBS-*g*-MA blends. The value of $\eta_\infty$ increases inappreciably with $\Phi_d$ in the PBT/SEBS systems which indicates that the rheological structure is strengthened by SEBS, although marginally, probably through interdiffusion of the polymers at higher shear rates. In the compatibilized blends, the parameter also increased with $\Phi_d$, the values are higher than those in the PBT/SEBS blends which indicates that the rheological structure are stronger even at very high shear rate range due probably to enhanced phase adhesion in the compatibilized systems.

### Effect of Temperature on Melt Behaviour

The effect of temperature on the melt viscosity was obtained from semilogarithmic Arrhenius expression and the plot of log $\eta_a$ versus $1/T$ for the blends, Figure 9(A,B). $\Delta E$ values were evaluated from the slopes of these curves for PBT/SEBS and PBT/SEBS/SEBS-*g*-MA blends. The viscosity of the polymer melts decrease with increase in temperature because at higher temperatures the molecular motions are facilitated due to the free volume availability. The activation energy for viscous flow decreases with increase in $\Phi_d$, Table III, Figure 9(A), which implies that the free volume is not hindered by the presence of SEBS. In the PBT/SEBS/SEBS-*g*-MA blends, the $\Delta E$ also decreases with $\Phi_d$, Table III, Figure 9(B). It appears that the resistance to melt flow by the SEBS particles is offset by the plasticizing/lubricating effect of the compatibilizer.

### Melt Elasticity Parameters

On extrusion of a viscoelastic material through a capillary along with the axial stresses in the flow direction some stresses normal to the axial stress, known as normal stresses, are also generated. The normal stresses are due to the elastic nature of the melt and are manifested in the form of extrudate swell. This flow in the normal direction is retarded by the viscosity of the melt. The normal stresses were calculated from the extruded swell measurements following Tanner's equation:[37]

$$\tau_{11} - \tau_{22} = 2\tau_W[2(D_i/D)^6 - 2]^{1/2} \tag{10}$$

where $\tau_{11}-\tau_{22}$ (or $N_1$) is the first normal stress difference, and $D_i$ and $D$ are the diameters of the extrudate and the cappilary

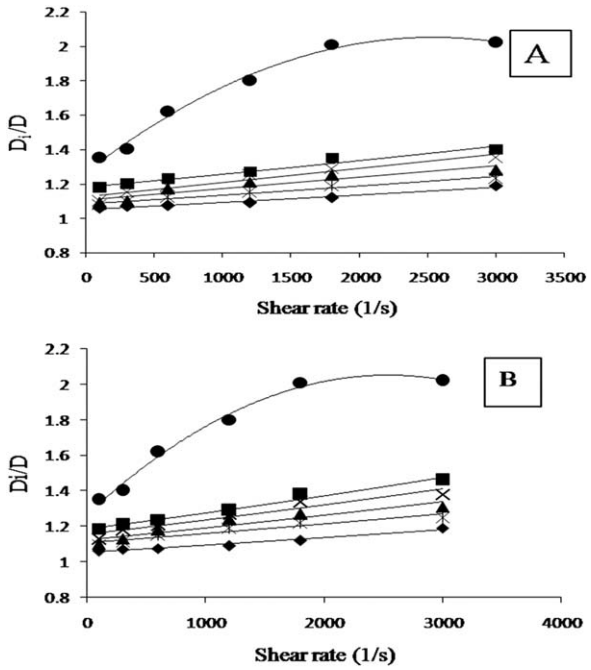


**Figure 10.** Variations of extrudate swell ratio, ($D_i/D$), versus shear rate of the (A) PBT/SEBS and (B) PBT/SEBS/SEBS-*g*-MA blends at varying $\Phi_d$ : 0 (◆), 0.07(∗), 0.14(▲), 0.26 (×), 0.38 (■), and 1(•).

die, respectively. Other elastic parameters were also calculated from the value of $N_1$. The recoverable shear strain ($\gamma_R$) or the Weissenberg number is defined by eq. (11):[38,39]

$$\Upsilon_R = \frac{N_1}{2\tau_W} \tag{11}$$

where $\tau_w$ is the shear stress at the capillary wall. The first normal stress co-efficient, $\psi_1$, also known as the elasticity function, is defined by:[40]

$$\Psi_1 = \frac{N_1}{\dot{\gamma}^2} \tag{12}$$

The parameter $\psi_1$ is strongly dependent on shear rate and may be expressed as:

$$\Psi_1 = \Psi_1^0 \cdot \dot{\gamma}^{(m-2)} \tag{13}$$

where, $\psi_1^0$ is the standardized elasticity and $m$ the elasticity exponent. Shear compliance of the melt is written as:[38,39]

$$J_S^O = \frac{N_1}{2\tau_W{}^2} \tag{14}$$

while relaxation time, $\lambda$, can be expressed as:[40]

$$\lambda = \frac{\Psi_1(\dot{\gamma})}{2\eta(\dot{\gamma})} \tag{15}$$

Strain on capillary wall ($F$) can be expressed as eq. (16):[40,41]

$$F = \frac{3n+1}{2(5n+1)} \tag{16}$$

### Extrudate Swell Ratio

The melt elasticity parameter extrudate swell ratio, $D_i/D$, of the PBT/SEBS and PBT/SEBS/SEBS-*g*-MA blends are presented in Figure 10(A,B). The $D_i/D$ values of neat PBT, SEBS and the blends enhance with shear rate, Figure 10(A), the degree of enhancement of the parameter for elastomer was significantly higher than that of PBT since the elastomer was more elastic than PBT. The values for the blends lie between the neat polymers since the elasticity is enhanced depending on the concentration of the dispersed phase. The $D_i/D$ values of the PBT/SEBS/SEBS-*g*-MA blends were higher to an extent than those of the uncompatibilized blends, Figure 10(B), which may be attributed to enhanced elasticity in the blends due to increased phase adhesion in presence of the compatibilizer.

### Elasticity Function of the Blends

The variations of elasticity function $\psi_1$ i.e. the first normal stress coefficient of PBT/SEBS blends versus $\dot{\gamma}$ are shown in Figure 11(A). The values decrease with increase in $\dot{\gamma}$ in all the blends. The values of $\psi_1$ of the blends were significantly higher than those of unblended PBT. This increase can be attributed to the presence of the elastomer for which the elasticity function is very high, Figure 11(B), this also indicates that the relaxation of the elastomer is very slow than PBT and the PBT/SEBS blends.

The elasticity function $\psi_1$ is expressed as a function of shear rate, eq. (13), where the elastic exponent m measures melt elasticity and the standardized elasticity $\psi_1^0$ is indicative of the modulus of elasticity of the melt.[40] Table IV presents the elastic parameters of PBT/SEBS blends. The elastic exponent is the highest for SEBS polymer which is quite expected because the polymer is highly elastic while the exponent values for the PBT/SEBS blends and PBT are less. Similarly the standardized elasticity $\psi_1^0$ is significantly high for SEBS copolymer compared to the data for PBT and the PBT/SEBS blends which is again due to the higher elasticity of the elastomer.

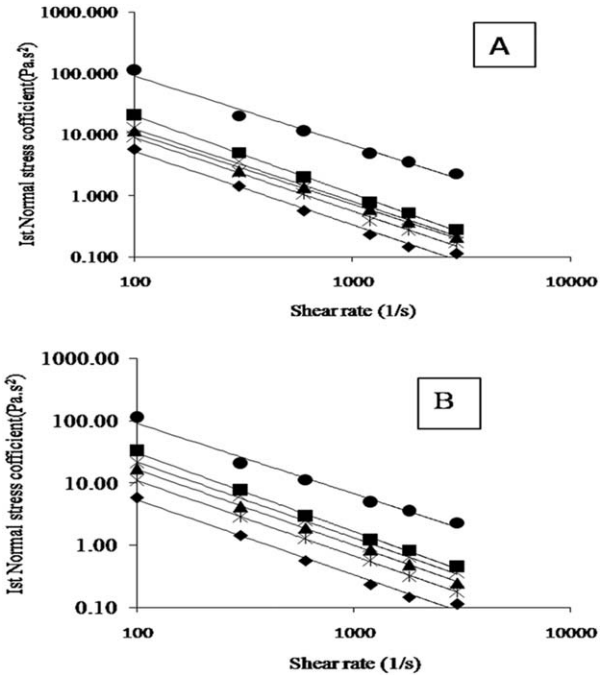


**Figure 11.** Variations of $\psi_1$ (first normal stress coefficient) versus shear rate ($\dot{\gamma}$) of (A) PBT/SEBS and (B) PBT/SEBS/SEBS-*g*-MA blends at varying $\Phi_d$: 0 (◆), 0.07(∗), 0.14(▲), 0.26 (×), 0.38 (■), and 1 (•).

**Table IV.** Elasticity Functions of Uncompatibilized and Compatibilized PBT and SEBS Blends

| Blend | Volume fraction | Elasticity function $\Psi 1 = \Psi 1^{\circ}\ \dot{\gamma}^{(m-2)}$ | Elasticity component (m) | Standardized elasticity ($\Psi 1o()$ |
|---|---|---|---|---|
| | 0 | $1{,}333\,\dot{\gamma}^{0.8-2}$ | 0.8 | 1,333 |
| PBT/sebs blends | 0.07 | $2{,}245\,\dot{\gamma}^{0.8-2}$ | 0.8 | 2,245 |
| | 0.14 | $2{,}198\,\dot{\gamma}^{0.84-2}$ | 0.84 | 2,198 |
| | 0.26 | $2{,}905\,\dot{\gamma}^{0.82-2}$ | 0.82 | 2,905 |
| | 0.38 | $7{,}069\,\dot{\gamma}^{0.73-2}$ | 0.73 | 7,069 |
| | 1 | $16{,}377\,\dot{\gamma}^{0.88-2}$ | 0.88 | 16,377 |
| PBT/SEBS/SEBS-*g*-MA | 0 | $1{,}333\,\dot{\gamma}^{0.8-2}$ | 0.8 | 1,333 |
| | 0.07 | $2{,}916\,\dot{\gamma}^{0.79-2}$ | 0.79 | 2,916 |
| | 0.14 | $4{,}753\,\dot{\gamma}^{0.78-2}$ | 0.78 | 4,753 |
| | 0.26 | $5{,}919\,\dot{\gamma}^{0.79-2}$ | 0.79 | 5,919 |
| | 0.38 | $10{,}471\,\dot{\gamma}^{0.74-2}$ | 0.74 | 10,471 |
| | 1 | $16{,}377\,\dot{\gamma}^{0.88-2}$ | 0.88 | 16,377 |

The variations of $\psi_1$ with $\dot{\gamma}$ in the PBT/SEBS/SEBS-*g*-MA blends are quite similar as in the PBT/SEBS blends, the values at corresponding $\Phi_d$ values are significantly higher, Figure 11(B), Table IV. The m values are marginally lower than the uncompatibilized blends. However the standardized elasticity $\psi_1^0$ values are significantly higher than the PBT/SEBS system which is due to enhanced consistency of the blends arising out of phase adhesion in presence of the compatibilizer.

### Recoverable Shear Strain, $\gamma_R$

The variations of $\gamma_R$, eq. (11), as functions of shear stress ($\tau_w$) are presented in Figure 12(A,B) for the PBT/SEBS and PBT/SEBS/SEBS-*g*-MA blends. For PBT the parameter enhances with shear stress, for SEBS the parameter increases to a much greater extent. Both types of blends exhibit enhanced recovery, the data lie between the plastic and elastomeric materials. This implies that the blends recover quite easily the induced strain in them, the recovery being quicker at higher shear stresses. In the compatibilized blends the recovery values are to a degree higher at corresponding shear stresses which may be due to enhanced phase adhesion.

### Relaxation Time ($\lambda$)

Figure 13(A,B) exhibit the variations of the parameter $\lambda$ versus $\gamma^{\bullet}$, eq. (15). The relaxation time for the PBT/SEBS and

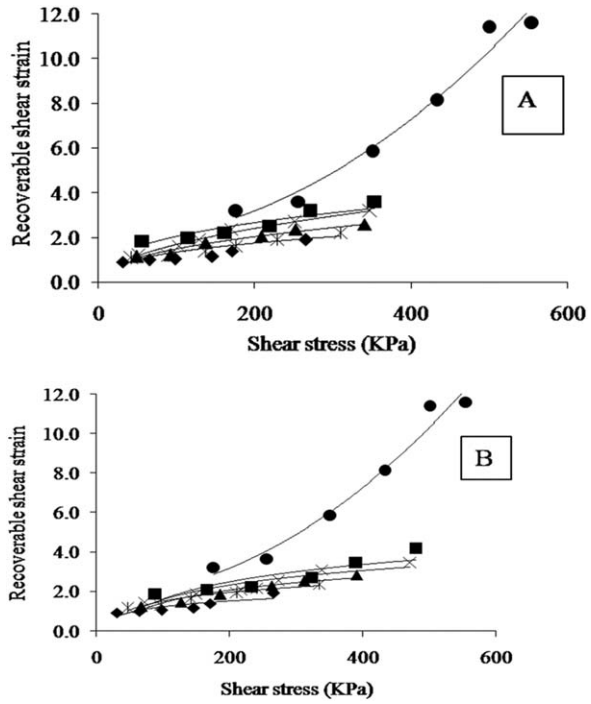


**Figure 12.** Variations of recoverable shear strain ($\gamma_R$) versus shear stress ($\tau$) for (A) PBT/SEBS and (B) PBT/SEBS/SEBS-*g*-MA blends at varying $\Phi_d$ : 0 (◆), 0.07(∗), 0.14(▲), 0.26 (×), 0.38 (■), and 1 (•).

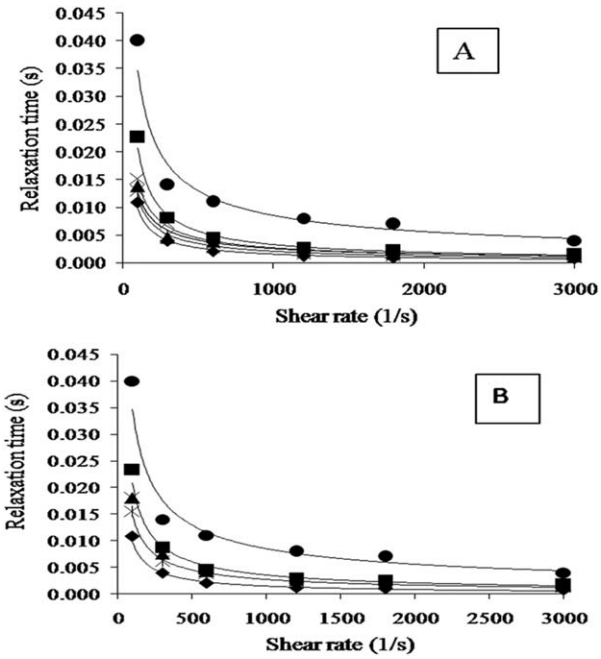


**Figure 13.** Variations of relaxation time ($\lambda$) versus shear rate ($\dot{\gamma}$) for (A) PBT/SEBS and (B) PBT/SEBS/SEBS-*g*-MA blends at varying $\Phi_d$ : 0 (◆) 0.07(∗), 0.14(▲), 0.26 (×), 0.38 (■), and 1(•).

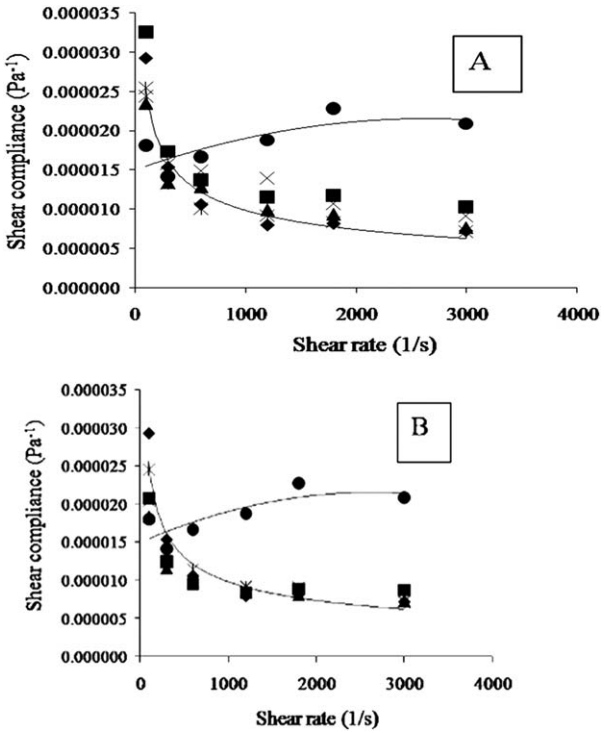


**Figure 14.** Variations of shear compliance ($J_c$) versus shear rate ($\dot{\gamma}$) for (A) PBT/SEBS and (B) PBT/SEBS/SEBS-*g*-MA blends at varying $\Phi_d$ : 0(◆), 0.07(∗), 0.14(▲), 0.26 (×), 0.38 (■), and 1(•).

PBT/SEBS/SEBS-*g*-MA blends and the pure components decrease with increase in shear rate, the decrease is quite rapid up to shear rate 700 $s^{-1}$ and the decrease in relaxation time is only marginal at $\dot{\gamma} > 700$ $s^{-1}$. This means that at low $\dot{\gamma}$ values the polymers take longer time to relax whereas at higher $\dot{\gamma}$ values the polymers and blends relax quickly. The $\lambda$ values of PBT are the lowest due to quick relaxation by the polymer beyond its melting point whereas the relaxation for the more elastic SEBS is higher. The relaxation time of the compatibilized blends are to a degree higher than the PBT/SEBS blends at corresponding $\Phi_d$ and $\dot{\gamma}$ values, which may be due to restriction to the relaxation arising out of enhanced phase adhesion.

### Shear Compliance

Shear compliance, $J_s^\circ$, eq. (14), is the reciprocal of shear modulus of a fluid and is indicative of fluidity or flow ability of the material. While the shear compliance in a polymer depends on the molecular weight, molecular weight distribution and entanglement density in the polymer, in a polymer blend the parameter is governed by additional factors e.g. dispersion of the discrete phase and phase adhesion, if any. Figure 14(A,B) exhibit the variations of $J_s^\circ$ values against $\dot{\gamma}$. The shear compliance values for SEBS enhance marginally with shear rate, Figure 14(A), the values for PBT and PBT/SEBS blends decrease quite rapidly up to $\sim\dot{\gamma} = 700$ $s^{-1}$ and beyond this shear rate the values become almost constant implying orientation and alignment of the polymer molecule. The compliance data for PBT are lower than the blends at all the $\dot{\gamma}$ values. This is because the elastomer, although highly elastic, enhances the fluidity of the blends.

In the PBT/SEBS/SEBS-*g*-MA blends quite similar variations of the shear compliance were observed, Figure 14(B). The parameters for the blends were higher than those of PBT; however the values were a degree lower than those in the uncompatibilized blends at corresponding $\Phi_d$ values. Enhancement of chain entanglements arising out of increased phase adhesion may be attributed to the decreased shear compliance (i.e. increased shear modulus) in these blends.

### Strain on the Capillary Wall

When processed the materials will induce some strain on the processing equipment depending upon the shear acting on them under the processing conditions. Similarly, the material, when extruded through a capillary, will exert some strain on the capillary wall, where the shear stress is maximum. The strain on the capillary wall ($F$) was estimated from the flow behaviour index ($n$) value using eq. (16). The strain on the capillary wall induced by the compatibilized and uncompatibilized blend as functions of $\Phi_d$ are shown Figure 15. The $F$ values decreased with increase in $\Phi_d$. the data were lower for the compatibilized blends than PBT/SEBS blends. When the volume fraction of the elastomer increases in the uncompatibilized blends, the flowability component in the molten material also increases (decrease in $n$ value) giving low $F$ values (since the denominator is higher for any value of n) which exerts less strain on the wall of the capillary. In the PBT/SEBS/SEBS-*g*-MA blends the increase in flowability component is to an extent higher which may be due to the predominance of plasticizing/lubricating function by the lower molecular weight fractions of SEBS-*g*-MA copolymer compared to the phase adhesion reducing the induced elastic strain on the capillary wall.

## CONCLUSION

In the PBT/SEBS blends the shear stress increases with the SEBS concentration as well as shear rate. The melt viscosity of the blends also increases with the SEBS content in PBT/SEBS and PBT/SEBS/SEBS-*g*-MA blend systems. The power law exponent and the consistency index decrease and increase, respectively, with increase in the $\Phi_d$. Consistency index values are higher for compatibilized system. The dynamic interfacial tension between

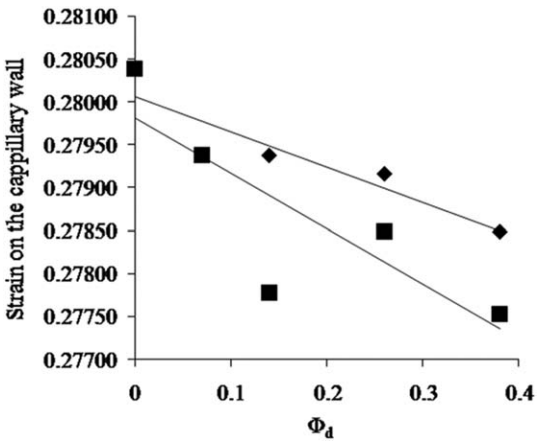


**Figure 15.** Plots of strain on capillary wall versus $\Phi_d$ for PBT/SEBS (◆) and PBT/SEBS/SEBS-*g*-MA (■) blends.

the component polymers was reduced in presence of the compatibilizer SEBS-*g*-MA, which stabilized the dispersed phase in the compatibilized blends. Activation energy decreases in both the blends, the decrease was higher in the compatibilized systems due to predominating plasticizing/lubricating effect of low molecular weight SEBS-*g*-MA copolymers over phase adhesion.

The first normal stress coefficient functions for all the uncompatibilized and compatibilized blends decrease with increasing shear rate. The recoverable shear strain and the relaxation behavior of the PBT/SEBS blends were quite low due to the phase continuity in the system. However, compatibilized blends exhibit good recoverability due to enhanced phase continuity on account of a degree of phase adhesion. The shear compliance values of the compatibilized blends were comparatively low than those of the corresponding uncompatbilized blends due to enhanced phase adhesion. Strain at capillary wall decreases in both the blends, the decrease was higher in the compatibilized systems due to predominating plasticizing/lubricating effect of low molecular weight SEBS-*g*-MA copolymers over phase adhesion.

## ACKNOWLEDGMENTS

The authors are thankful to (IRD) for research grant and Senior Research Fellowship to one of them (R.S.).

## REFERENCES

1. Paul, D. R; Newman, S. Polymer Blends; Academic Press: New York, **1978**; Vol. *2*, p 35.
2. Chirawithayaboon, A.; Kiatkamjornwong, S. *J. Appl. Polym. Sci.* **2004**, *91*, 742.
3. Bucknall, C. B. Toughening Plastic; Applied Science Publishers: London, **1977**; p 19.
4. Margolina, A.; Wu, S. H. *Polymer* **1988**, *29*, 2170.
5. Wu, S. H. *Polymer* **1985**; *26*, 1855.
6. Margolina, A.; Wu, S. H. *Polymer* **1990**, *31*, 972.
7. Kimura, M.; Porter, R. S. *J. Polym. Sci. Part B: Polym. Phys.* **1983**, *21*, 367.
8. Mencik, Z. *J. Polym. Sci. Part B: Polym. Phys.* **1975**, *13*, 2173.
9. Martin, P.; Devaux, J.; Legras, R.; vanGurp, M.; vanDuin, M. *Polymer* **2001**, *42*, 2463.
10. Sharma, R.; Maiti, S. N. *Polym. Eng. Sci.* **2013**, *53*, 2242.
11. Lu, M.; Keskkuula, H.; Paul, D. R. *Polym. Eng. Sci.* **1994**, *34*, 33.
12. Majumdar, B.; Keskkula, H.; Paul, D. R. *Polymer* **1994**, *35*, 1386.
13. Sanchez-Solis, A.; Calderas, F.; Manero, O. *Polymer* **2001**, *42*, 7335.
14. Asthana, H.; Jayaraman, K. *Macromolecules* **1999**, *32*, 3412.
15. Liu, S.; Qin, S.; Luo, Z; Yu, J.; Guo, J.; He, M. *J. Macromol. Sci. Part B: Phys.* **2011**, *50*, 1780.
16. Yao, Z.; Lin, M.; Zhou, J.; Wang, H.; Zhong, W.; Du, Q. *Polym. Eng. Sci.* **2007**, *47*, 1943.
17. Verma, G.; Kulshreshtha, B.; Tyagi, S.; Ghosh, A. K. *Polym. Plast. Technol. Eng.* **2008**, *47*, 969.
18. Rosand RH7 User Mannual; Malvern Instruments Ltd.: Worcestershire: UK, **2006**.
19. Leblans, J. R.; Sampers, J.; Booj, H. C. *Rheol. Acta.* **1985**, *24*, 152.
20. Dealy, J. M.; Wissbrun, K. F. Melt Rheology and its Role in Plastics Processing: Theory and Applications; Kluwer Academic Publishers: New York, **1999**.
21. Ferguson, J.; Kemblowski, Z. Applied Fluid Rheology; Elsevier: Amsterdam, **1991**.
22. Laun, H. M. *Rheol. Acta* **2004**, *43*, 509.
23. Gupta, R. K.; Nielsen, L. E. Polymer and Composite Rheology; Marcel Dekker: New York, **2000**.
24. Brydson, J. A. Flow Properties of Polymer Melts; Iliffe: London, **1978**.
25. Middleman, S. The Flow of High Polymers; Continuum and Molecular Rheology; Wiley-Interscience: New York, **1968**.
26. Mckelvy, J. M. Polymer Processing; Wiley: New York, **1962**.
27. Balamurugan, G.; Prasath, M. S. N. *Polym. Eng. Sci.* **2008**, *48*, 2482.
28. Martuscelli, E.; Silvestre, C.; Abote, G. *Polymer* **1982**, *42*, 229.
29. Gupta, A. K.; Kumar, P. K.; Ratnam, B. K. *J. Appl. Polym. Sci.* **1991**, *42*, 2595.
30. Taylor, G. I. *Proc. R. Soc.* **1932**, *41*, A138.
31. Taylor, G. I. *Proc. R. Soc.* **1934**, *501*, A146.
32. Choi, G. D.; Jo, W. H.; Kim, H. G. *J. Appl. Polym. Sci.* **1996**, *59*, 443.
33. Huitric, J.; Moan, M.; Carreau, P. J.; Dufaure, N. *J. Non-Newt. Fluid Mech.* **2007**,*145*, 139.
34. Sewda, K.; Maiti, S. N. *Polym. Plast. Technol. Eng.* **2010**, *49*, 418.
35. Vanoene, H. *J. Colloid Interface Sci.* **1972**, *40*, 448.
36. Casson, N. In Proceedings of the Conference of the British Society of Rheology, University College, Swansea; Pergamon: London, **1957**.
37. Tanner, R. I. *J. Polym. Sci. Part A-2: Polym. Phys.* **1970**, *8*, 2067.
38. Chohan, R. K. *J. Appl. Polym. Sci.* **1994**, *54*, 487.
39. Chohan, R. K. *J. Appl. Polym. Sci.* **1995**, *56*, 1455.
40. Plochocki, A. P. *Adv. Polym. Tech.* **1982**, *2*, 267.
41. Utracki, L. A.; Weiss, R. A. Eds. ACS Symposium Series; American Chemical Society: Washington, DC., **1989**.